# Simulation of Indirect-Direct Transformation Phenomenon of Germanium under Uniaxial and Biaxial Strain along Arbitrary Orientations

Ziyang Xiao and Neil Goldsman
Department of Electrical and Computer Engineering
University of Maryland
College Park, Maryland 20742
Email: chrisx29@umd.edu

Nibir K. Dhar
CERDEC
Night Vision and Electronic Sensors Directorate
Fort Belvoir, VA 22060

***Abstract*—Germanium can be transformed from an indirect bandgap material to a direct bandgap material by applying strain. Unstrained Ge has an indirect bandgap of 0.66eV (at L point) and a direct bandgap of 0.8eV [1]. When strain is applied, the band structure of germanium will be altered. When the strain is tensile, both the indirect and the direct bandgaps tend to decrease. Under certain strains, the direct bandgap will be pushed even below the indirect bandgap, at which point, germanium becomes a direct bandgap material. The value of the bandgap when Ge transforms from an indirect to direct semiconductor upon the application of strain is named the Bandgap Transition Point (BTP), and the required strain is named STP (Strain at Transition Point). Previous research has been done on uniaxial and biaxial strained germanium on the conventional orientations. In this work, calculations are made on the effect of applying tensile stress in arbitrary orientations based on nonlocal empirical pseudopotential method (EPM) [2] [3]. We also use cubic spline interpolation of the atomic form factors [4] [5], as well as the rules for strain translation [6], to determine how the Indirect-Direct transformation phenomenon of germanium changes with respect to virtually any orientation of the crystal planes. In addition, we calculated the optimal orientation and the effect that departure from this optimal orientation has on the bandgap.**

## I. Introduction

Germanium has re-drawn attention in the realm of photo detecting in the Short Wave Infrared (SWIR) range because of its advantage of being well suited to be integrated into a CMOS process, as well as having direct bandgap of 0.8eV and indirect bandgap of 0.66eV, with the difference between the two being only 0.14eV. Former research has pointed out the band structure of germanium can be altered by applying strain [1]. Additionally, the direct bandgap and indirect bandgap react differently to the applied strain. Previous work has been done to reveal the relationship between germanium band structure and the applied strain, that tensile strain (whether uniaxial, biaxial or hydraulic) will help decrease the difference between the direct and indirect bandgap, and eventually transform germanium into a direct bandgap material. Such conclusion has been mainly made towards most common orientations of the germanium material. However, considering the possible error happening during the manufacturing process, there may be shifting of the strain applied direction or plane. In this paper, simulations have been conducted to look into the relationship between the bandgap transition point (BTP) (when germanium turns into direct bandgap material at what strain) and arbitrary orientation (plane for biaxial strain and direction for uniaxial strain) of the applied strain.

## II. Empirical Pseudopotential Method

The whole method starts with a plane wave expansion, from which the total wave function solution of the Schrödinger Equation is taken to be sum of a series of orthogonalized plane wave functions. Under the expansion, the differential Schrödinger Equation is transferred into an algebra equation expressed as Equation (1) [3]:

$$\left\{\left[\frac{k^2(\vec{k}+\vec{G})^2}{2m}\right]+\sum_{\vec{G}'}V(\vec{G}-\vec{G}')\right.$$
$$\left.\sum_{\vec{G}'}V_{ps}^{NL}(\vec{k},\vec{G},\vec{G}')\right\}=E\cdot U(\vec{G}) \quad (1)$$

Where:

$\vec{G}$ is the vector of the reciprocal lattice points

$V(\vec{G})$ is the Fourier transformation coefficient of the periodic nuclei potential)

$U(\vec{G})$ is the Fourier transformation coefficient of the Bloch function)

$V_{ps}^{NL}$ is the inclusion of the nonlocal effects of different orbitals feeling different pseudopotential within the core region.

For elemental crystals like germanium and silicon, the Fourier transformation coefficient of the potential V($\vec{G}$) is expressed as:

$$V(\vec{G})=cos\frac{\vec{G}\cdot\vec{r_b}}{2}V_s(\vec{G}) \quad (2)$$

Where:



978-1-4673-7860-4/15/$31.00 ©2015 IEEE

TABLE I. COEFFICIENT FOR LOCAL PSEUDOPOTENTIAL METHOD AND FOR NONLOCAL COMPENSATION [2] [3]

| local coefficient:Form factor(Ry) | | | | |
|---|---|---|---|---|
| $V(\sqrt{3})$ -0.221 | | $V(\sqrt{8})$ 0.019 | $V(\sqrt{11})$ 0.056 | |
| Nonlocal coefficient | | | | |
| $\alpha_0(Ry)$ | $\beta_0$ | $A_2(Ry)$ | Radii(A) | |
| | | | $R_0$ | $R_2$ |
| 0 | 0 | 0.275 | 0 | 1.22 |

$\vec{r_b}$ is the vector of the basis of the germanium lattice

$V_s(\vec{G})$ is the form factor, indicating the potential in the reciprocal space.

By choosing N bases of the wave function (the number of $V(\vec{G})'s$), Equation (1) will be further transformed into a matrix equation, with the size of N×N. To restore the real wave function, number N would be extremely huge due to the rapid changing atomic potential at the core region, which results in a high calculation expenses.

However, by replacing the rather rapidly changing all-electron potential with a smooth pseudopotential, the number of wave planes needed will be greatly reduced, which, to be more specific, will be 51 in total in our case with $|\vec{G}|^2 \leq 11$. In Table I, the form factors needed to construct the valence electron band structure are listed along with the coefficients for nonlocal compensation.

## III. STRAIN COORDINATE SYSTEM TRANSFORMATION

From the view of a more practical consideration, the types of strain that are usually applied are 1) uniaxial: applying strain along a certain direction, typically in a nanowire structure and 2) biaxial: applying strain on a certain plane, typically in a deposited film. For crystals with a cubic lattice structure like germanium, the two basic strain types can be simply expressed by a diagonal tensor, as in:

$$\bar{\bar{\epsilon}}'(\overline{x'y'z'}) = \begin{pmatrix} \epsilon_{x'x'} & 0 & 0 \\ 0 & \epsilon_{y'y'} & 0 \\ 0 & 0 & \epsilon_{z'z'} \end{pmatrix} \tag{3}$$

The coordinate system used in Equation (3) (expressed as $\overline{\overline{x'y'z'}}$) is considered as arbitrary, which is not necessarily aligned with the one used in the statement in the previous section (expressed as $\overline{\overline{xyz}}$, whose x axis is aligned with [100], y aligned with [010] and z aligned with [001]). Therefore, a coordinate system transformation is needed to project the initially applied strain under $\overline{\overline{x'y'z'}}$ onto $\overline{\overline{xyz}}$. In other words, we already have $\bar{\bar{\epsilon}}(\overline{x'y'z'})$, and we need to obtain $\bar{\bar{\epsilon}}(\overline{xyz})$.

To achieve this we apply a linear transformation tensor $\overline{\overline{T}}$, which allows us to work in the coordinate systems where the axes are aligned with the family of $\langle 100 \rangle$ directions. Tensor $\overline{\overline{T}}$ is expressed in Equation (4):

$$\overline{\overline{x'y'z'}} = \overline{\overline{T}} \cdot \overline{\overline{xyz}} \tag{4}$$

The connection between stress tensors $\bar{\bar{\sigma}}(\overline{xyz})$ and $\bar{\bar{\sigma}}(\overline{x'y'z'})$ is then built by the expression:

$$\bar{\bar{\sigma}}(\overline{xyz}) = \overline{\overline{T}}^T \cdot \bar{\bar{\sigma}}(\overline{x'y'z'}) \cdot \overline{\overline{T}} \tag{5}$$

Under both coordinate systems, the strain and stress vectors obey the Hooke's Law, as in:

$$\vec{\sigma}(\overline{x'y'z'}) = \bar{\bar{c}}(\overline{x'y'z'}) \cdot \vec{\epsilon}(\overline{x'y'z'}) \tag{6}$$
$$\vec{\sigma}(\overline{xyz}) = \bar{\bar{c}}(\overline{xyz}) \cdot \vec{\epsilon}(\overline{xyz}) \tag{7}$$

Therefore, through Equation (6) and Equation (5), we are able to get the stress vector $\vec{\sigma}(\overline{xyz})$. Then through Equation (7), the stress is ultimately transformed into the strain vector $\vec{\epsilon}(\overline{xyz})$.

In Equation (6) and Equation (7), $\bar{\bar{c}}(\overline{xyz})$ is the stiffness matrix under $\overline{xyz}$, whereas $\bar{\bar{c}}(\overline{x'y'z'})$ is the stiffness matrix under $\overline{x'y'z'}$, whose terms can be expressed in terms of elements in $\bar{\bar{c}}(\overline{xyz})$ [6]:

$$c'_{11} = c_{11} + c_e(l_1^4 + m_1^4 + n_1^4 - 1) \tag{8}$$
$$c'_{12} = c_{12} + c_e(l_1^4 + m_1^4 + n_1^4 - 1) \tag{9}$$
$$c'_{44} = c_{11} + c_e(l_1^4 + m_1^4 + n_1^4 - 1) \tag{10}$$
$$c'_{14} = c_{11} + c_e(l_1^4 + m_1^4 + n_1^4 - 1) \tag{11}$$

Where:

$$c_e = c_{11} - c_{12} - 2c_{44}$$
$$l_1 = cos(xx'), l_2 = cos(xy'), l_3 = cos(xz')$$
$$m_1 = cos(yx'), m_2 = cos(yy'), m_3 = cos(yz')$$
$$n_1 = cos(zx'), n_2 = cos(zy'), n_3 = cos(zz')$$

Also, $c'_{11}$ is analogous to $c'_{22}$ and $c'_{33}$. $c'_{12}$ is analogous to $c'_{13}$ and $c'_{23}$. $c'_{44}$ is analogous to $c'_{55}$ and $c'_{66}$. While $c'_{14}$ is analogous to $c'_{15}$, $c'_{16}$, $c'_{24}$, $c'_{25}$, $c'_{26}$, $c'_{34}$, $c'_{35}$, $c'_{36}$, $c'_{45}$, $c'_{46}$ and $c'_{56}$

During the projection process, the conversion between the tensor form and the vector form of a certain stress or strain is used wherever necessary.

## IV. STRAINED LATTICE AND RECIPROCAL LATTICE

After the projection of the strain tensor $\bar{\bar{\epsilon}}'$ under $\overline{\overline{x'y'z'}}$ onto $\bar{\bar{\epsilon}}$ under $\overline{\overline{xyz}}$, the primitive lattice vector is distorted as follows:

$$\vec{a_i}' = (\bar{\bar{1}} + \bar{\bar{\epsilon}}) * \vec{a_i} \tag{12}$$

Where: $i = 1, 2, 3.$

The new reciprocal lattice vector will be distorted as well by:

TABLE II. INTERPOLATION PARAMETERS FOR CONTINUOUS $V(|G|)$ VS. $|G|$ CURVE

| Parameter | Value (in atomic value) |
|---|---|
| $C_1$ | 23.31608 |
| $C_2$ | 2.50648 |
| $C_3$ | 0.63901 |
| $C_4$ | 0.97655 |
| $C_5$ | 5.0 |
| $C_6$ | 0.3 |

$$\vec{G_1}' = 2\pi \frac{\vec{a_2}' \cdot \vec{a_3}'}{\vec{a_1}' \cdot (\vec{a_2}' \cdot \vec{a_3}')} \tag{13}$$

$$\vec{G_2}' = 2\pi \frac{\vec{a_3}' \cdot \vec{a_1}'}{\vec{a_1}' \cdot (\vec{a_2}' \cdot \vec{a_3}')} \tag{14}$$

$$\vec{G_3}' = 2\pi \frac{\vec{a_1}' \cdot \vec{a_2}'}{\vec{a_1}' \cdot (\vec{a_2}' \cdot \vec{a_3}')} \tag{15}$$

$$\tag{16}$$

For the strained germanium lattice, the discrete form factor is expanded into a continuous curve and the values are interpolated using cubic splines by the expression [7].:

$$V(|\vec{G}|) = \frac{1}{\Omega} \frac{C_1(|\vec{G}|^2 - C_2)}{exp\left[C_3(|\vec{G}|^2 - C_2) - 1\right]} \left[\frac{1}{2} tanh(\frac{C_5 - |\vec{G}|^2}{C_6}) + \frac{1}{2}\right] \tag{17}$$

where:

$\Omega$ is the atomic volume of the primitive unit cell.

$C_1 - C_6$ are interpolation parameters to fit the local form factor values, which are listed in Table II [7]. Adjustment of the interpolation parameters has been made to fit the values listed in Table I.

## V. SIMULATION RESULTS AND ANALYSIS

As was mentioned before, because of the applied strain, the lattice, as well as the reciprocal lattice, will be distorted. Therefore, the originally equivalent high symmetry points in k-space may no longer be equivalent under the influence of the strain. To be more specific, the eight L points in the first Brillouin Zone may have different energy levels under the influence of the applied strain. In Figure 1, we can see the non-equivalence of the L points in the conduction band, with the case of biaxial strain on $\{111\}$ plane having a 2:6 split between the eight L points in the conduction band (the upper right L valley is lower than the other three), and in the case of biaxial strain on $\{110\}$ they have a 4:4 split (the antidiagonal two L valleys are lower than the diagonal two). Furthermore, only the lowest of the eight points is considered the upper border of indirect bandgap. Therefore, a thorough investigation of all eight L points in the conduction band is necessary to find out the real, direct-indirect transformation point for any specific strain case.

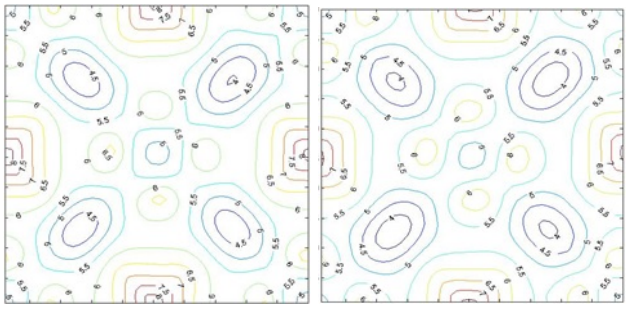

Fig. 1. Contour of conduction band on the plane in the reciprocal space passing through all four L points with kz = $\pi$/a. Left: biaxial strain on $\{111\}$ plane; Right: biaxial strain on $\{110\}$ plane

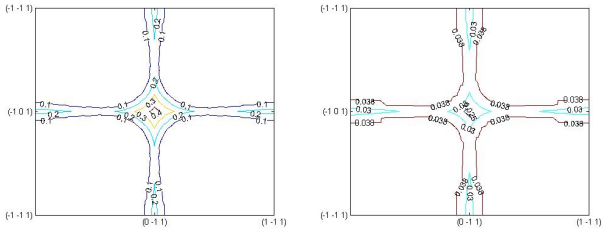

Fig. 2. Remaining Energy Band (BTP) (Left) and Required Strain (STP) (Right) at the transition point with respect to different orientations of the plane under biaxial strain. The value of contour curve represents the value of the BTP (left) or STP (right) at that point. Each point in the graph is a specific orientation. The center of the graph has Miller Index of (001). The corners are of the $\{111\}$ family and the mid-point of the sides are of the $\{110\}$ family.

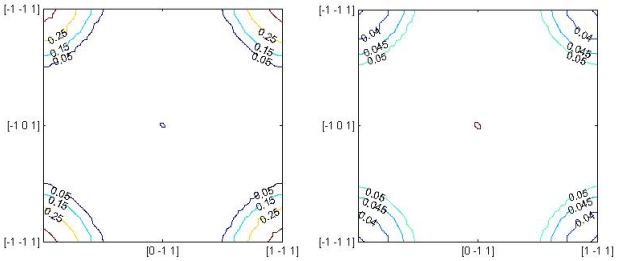

Fig. 3. BTP (Left) and STP (Right) with respect to different orientations of the crystal direction under uniaxial strain. The center of the graph is the direction with Miller Index of [001]. The corners are of the $\langle 111 \rangle$ family and the mid-point of the sides are of the $\langle 110 \rangle$ family.

Based on the method described above, Calculations of germanium under biaxial and uniaxial strain under arbitrary orientation are conducted, and the simulation results are shown in Figure 2 (for biaxial strain) and in Figure 3 (for uniaxial strain). From the graphs, one of the primary items that can be identified is the optimal orientation for each type of strain. This optimal orientation is defined as the one along which the achieved bandgap transition point has the largest resulting direct gap, and requires the least of strain.

The simulation results shown in Figures 2 and 3 clearly show the optimal orientations for both biaxial and uniaxial strain cases, $\{100\}$ plane (with BTP of 0.43eV and STP of 2.3%) and $\langle 111 \rangle$ direction (with BTP of 0.41eV and STP of

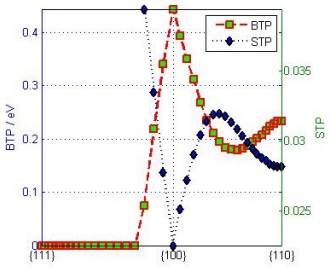


Fig. 4. BTP (left) and STP (right) under biaxial strain. The middle is the optimal plane $\{100\}$, to the left of the graph towards $\{111\}$ and to the right towards $\{110\}$.

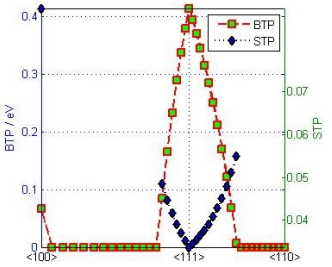


Fig. 5. BTP (left) and STP (right) under uniaxial strain. The middle is the optimal direction $\langle 111 \rangle$, to the left of the graph towards $\langle 100 \rangle$ and to the right towards $\langle 110 \rangle$.

3.4%), respectively. Additionally, the region with BTP of 0eV and the region with STP of more than 0.035(3.5%) in Figure 2 and 0.05(5%) in Figure 3, respectively, represent that under such orientation, no amount of strain can achieve the direct-indirect transformation before either the bandgap hits zero, or the conduction band at one or more of the eight L points is pushed below the valence band at the $\Gamma$ point. From roughly judging Figure 2 and Figure 3, the BTP and STP properties are highly sensitive to the orientation. To consider practically, this means that any tilting from the optimal orientation could possibly cause a significant difference on the requirement of achieving the direct-indirect transformation and on the amount of remaining bandgap. In addition to Figure 2 and Figure 3, Figure 4 and Figure 5 with more details are added showing the influence on BTP and STP when the material is tilted from the optimal orientations.

Figure 4 and Figure 5, respectively show how the direct-indirect transformation of germanium changes when the orientation of the applied strain is tilted from its optimal position. In both biaxial and uniaxial cases, as was mentioned before, the transformation property is quite sensitive to the tilting. For applying biaxial strain, when tilting away from the optimal orientation $\{100\}$ towards $\{111\}$, BTP decreases and STP increases drastically, with average slopes of 27.5meV/degree and 0.137% (strain)/degree and a cutoff angle of about $15.80^0$, beyond which there is no transition at any amount of strain. When tilting towards $\{110\}$ , the slopes for BTP and STP are only 14.8meV/degree and 0.060%(strain)/degree, respectively. However, on this tilting direction, the material is expected to always have transformation at sufficient amount of strain.

Similar results are obtained for uniaxial strain, when tilting from the optimal direction $\langle 111 \rangle$ towards $\langle 100 \rangle$, the average slopes of BTP and STP are 33.7meV/degree and 0.150% (strain)/degree, with cutoff angle of about $12.1^0$. While tilting towards $\langle 110 \rangle$, the slopes of BTP and STP are about 21.0meV/degree and 0.119% (strain)/degree, with the cutoff angle being $17.6^0$. Also at $\langle 100 \rangle$, transition is observed during simulation. However, this occurs at a relatively very high strain of about 9% and is extremely sensitive to any tilting from the orientation, behaving as an isolated point in the graph.

Both biaxial and uniaxial strain cases share the similarity for the Indirect-Direct transformation phenomenon around the optimal orientation, which is having a relatively high sensitivity on the error of the alignment with respect to the optimal orientation. Nonetheless, in the biaxial strain case, if the applied plane is not chosen as the optimal $\{100\}$ plane, but the $\{110\}$ plane, the transition curve of BTP and STP, as is shown in Figure 4, is smooth and flat, indicating a rather high stability against the possible error of the alignment along this specific orientation.

## VI. Conclusion

In conclusion, germanium's Direct-Indirect bandgap transformation phenomena under uniaxial and biaxial strain are investigated under arbitrary orientations. Calculations agree with previous research on the choice of optimal orientation for both strain cases, and in addition, we provide results about the sensitivity of the transformation property when the orientation of applied strain is tilted away from the optimal orientation. Both biaxial and uniaxial strain cases show high sensitivity against the alignment error. Furthermore, in the biaxial strain case, if the strain applied plane is chosen as $\{110\}$, a high tolerance is expected against the alignment error, which suggests a possible practical engineering application.

## References

[1] C. Boztug, J. R. Sánchez-Pérez, F. Cavallo, M. G. Lagally, and R. Paiella, "Strained-germanium nanostructures for infrared photonics," *ACS Nano*, vol. 8, no. 4, pp. 3136–3151, 2014, pMID: 24597822. [Online]. Available: http://dx.doi.org/10.1021/nn404739b

[2] M. L. Cohen and T. K. Bergstresser, "Band structures and pseudopotential form factors for fourteen semiconductors of the diamond and zinc-blende structures," *Phys. Rev.*, vol. 141, pp. 789–796, Jan 1966. [Online]. Available: http://link.aps.org/doi/10.1103/PhysRev.141.789

[3] J. R. Chelikowsky and M. L. Cohen, "Nonlocal pseudopotential calculations for the electronic structure of eleven diamond and zinc-blende semiconductors," *Phys. Rev. B*, vol. 14, pp. 556–582, Jul 1976. [Online]. Available: http://link.aps.org/doi/10.1103/PhysRevB.14.556

[4] S. Gonzalez, D. Vasileska, and A. Demkov, "Empirical pseudopotential method for the band structure calculation of strained silicon germanium materials," *Journal of Computational Electronics*, vol. 1, no. 1-2, pp. 179–183, 2002.

[5] J. Kim and M. Fischetti, "Empirical pseudopotential calculation of band structure and deformation potentials of biaxially strained semiconductors," in *Computational Electronics, 2009. IWCE '09. 13th International Workshop on*, May 2009, pp. 1–4.

[6] J. J. Wortman and R. A. Evans, "Young's modulus, shear modulus, and poisson's ratio in silicon and germanium," *Journal of Applied Physics*, vol. 36, no. 1, pp. 153–156, 1965. [Online]. Available: http://scitation.aip.org/content/aip/journal/jap/36/1/10.1063/1.1713863

[7] M. V. Fischetti and S. E. Laux, "Band structure, deformation potentials, and carrier mobility in strained si, ge, and sige alloys," *Journal of Applied Physics*, vol. 80, no. 4, 1996.